International Journal for Modern Trends in Science and Technology, 9(04): 06-11, 2023

ISSN: 2455-3778 online
DOI: https://doi.org/10.46501/IJMTST0904002
Available online at: http://www.ijmtst.com/vol9issue04.html

Artificial neural network control doubly fed induction generator based wind power system

[1]Praveena, [2]Pilla Venkatesh, [2]Thota Dinesh, [2]Lokarapu Surya Kumar, [2]Ranjith Kumar, [2]Indraganti Sudheer

[1]Assistant Professor, Dept of EEE, Avanthi Institute of Engineering and Technology, Vizianagaram
[2]Dept of EEE, Avanthi Institute of Engineering and Technology, Vizianagaram

To Cite this Article
Praveena, Pilla Venkatesh, Thota Dinesh, Lokarapu Surya Kumar, Ranjith Kumar, Indraganti Sudheer. Artificial neural network control doubly fed induction generator based wind power system. International Journal for Modern Trends in Science and Technology 2023, 9(02), pp. 06-11. https://doi.org/10.46501/IJMTST0904002

Article Info
Received: 02 March 2023; Accepted: 25 March 2023; Published: 29 March 2023.

ABSTRACT

Renewable energy sources (RES) are playing a vital role in fulfilling the future energy needs of the world. The modern power system architecture, which is power electronics based, entails numerous non-linear loads and distributed generations (RESs), resulting in the development of several PQ issues. This project proposes an Artificial Neural robust control method for a DFIG based wind energy conversion system. To reduce the chattering phenomena in the excitation system, advance controller system is employed for the adaptive adjustment of the discontinuous control gain while preserving the robustness of the closed-loop system. At first, the modelling of the turbine and the DFIG will be presented. Then, while using the proposed ANN controller, the rotor magnitudes are adjusted to accomplish vector control of the active and reactive power. The converter's goal is to operate at unity power factor and provide input currents with a tolerable harmonic content. At the interface between the powers electronic converter and the double fed induction generator (DFIG), extract the most real power possible. Finally, to validate the proposed controls, we will conduct a series of numerical simulations using MATLAB 2021a /Simulink software.

KEY WORDS: Wind System, DFIG, Power Transfer Matrix and ANN Controller

1. INTRODUCTION:

The electrical power generated by the wind system is one of the most reliable, efficient and developed renewable energy sources. The Doubly Fed Induction Generator is operated by a wind turbine with variable-speed variable-pitch control scheme. This system can be operated either grid connected mode or stand-alone mode. In present scenario the design of the wind turbine power plants is mainly depends on the DFIG technology. This a DFIG-based wind-power/storage system can deliver a specified amount of power to the grid, despite wind power fluctuations.

DFIG has two different control schemes stator flux reference frame used by for Rotor side control (RSC) is one and current reference frame used by Grid side control (GSC) is another to provide the firing pulses to the converters.

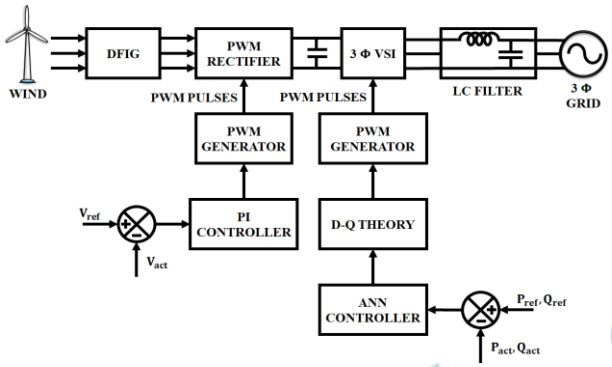

Figure 1: Schematic Diagram for DFIG based wind turbine

Figure 1 shows the schematic diagram for the wind turbine based doubly fed induction generator system. In this the stator is connected directly to the grid system and the rotor is controlled with the help of converters.

2. MODELLING AND DESIGN OF DFIG

The doubly fed induction generator is the better solution for variable speed machines with tolerance ±30% of synchronous speed. The grid and the rotor are directly connected for the main stator winding is controlled with converters via slip rings as sown in figure 2.

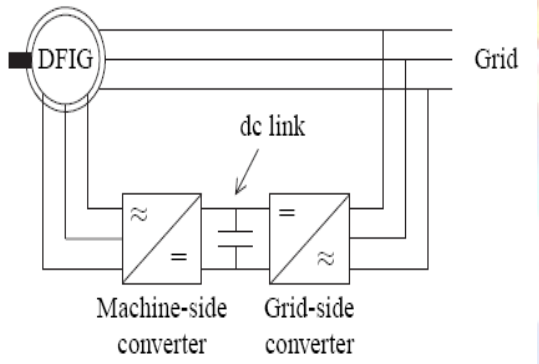

Figure 2: DFIG system with a Back-to-Back Converter

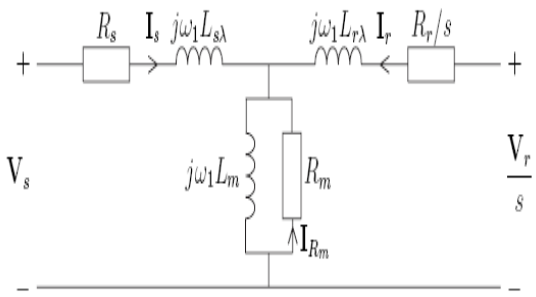

Figure 3: Equivalent circuit of DFIG

From application of Kirchhoff's voltage law applied to the above circuit 3, the voltage expressions for stator and rotor windings are expressed as,

$$Vs = j\omega_1 L_m (I_s + I_r + I_{Rm}) + j\omega_1 L_{s\lambda} I_s + R_s I_s \quad (1)$$

$$V_r/s = j\omega_1 L_m (I_s + I_r + I_{Rm}) + j\omega_1 L_{r\lambda} I_r + R_r/s * I_r \quad (2)$$

$$0 = j\omega_1 L_m (I_s + I_r + I_{Rm}) + R_m I_{Rm} \quad (3)$$

Rotor flux, stator flux, air-gap fluxes used in equations (1), (2) and (3) are defined below

$$\Psi_m = L_m (I_s + I_r + I_{Rm}) \quad (4)$$

$$\Psi_s = L_{s\lambda} I_s + \Psi_m = L_{s\lambda} I_s + L_m (I_s + I_r + I_{Rm}) \quad (5)$$

$$\Psi_r = L_{r\lambda} I_r + \Psi_m = L_{r\lambda} I_r + L_m (I_s + I_r + I_{Rm}) \quad (6)$$

The electro-mechanical torque is obtained from the above equations is expressed as

$$T_e = 3n_p I_m \Psi_r I_r^* = 3n_p I_m \Psi_m I^*_r \quad (7)$$

The rotor and stator powers are determined as

$$P_s = R_e [S_s] = 3R_s |I_s|^2 + 3R_m |I_{Rm}|^2 + 3\omega_1 I_m [\Psi_m I^*_r]$$

$$\approx 3\omega I_m [\Psi_m I^*_r] \quad (8)$$

$$P_r = R_e [S_r] = 3R_r |I_r|^2 - 3\omega_1 s I_m [\Psi_m I^*_r]$$

$$\approx -3\omega_1 s I_m [\Psi_m I^*_r] \quad (9)$$

From these DFIG mechanical power equations are calculated by

$$P_{mech} = 3\omega_r I_m [\Psi_m I^*_r] = 3\omega_1 I_m [\Psi_m I^*_r] - 3\omega_1 s I_m [\Psi_m I^*_r] \quad (10)$$

Wind-Turbine based doubly fed Induction Generator:

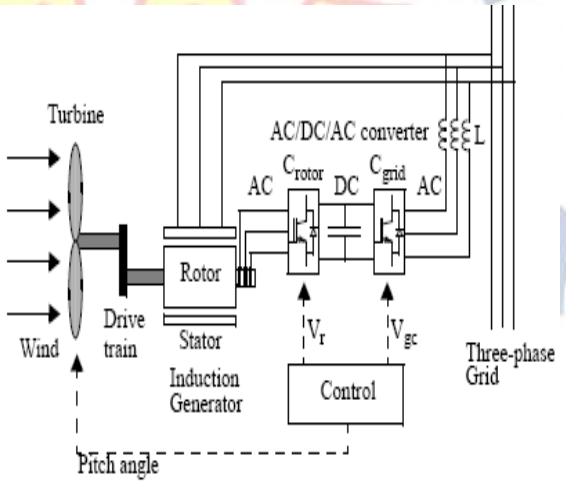

Figure 4: DFIG Connected to Wind Turbine

With the help of induction generator conversion of electrical energy from generated mechanical power from the wind blades and by the stator it is connected to the grid and the rotor converter terminals. Rotor voltage command signal Vr and grid command signal Vgc and the pitch angle command are generated by the control techniques and the respectively in order for controlling wind turbine power, the DC bus voltage between the rotor and stator converters and the voltage at the grid terminals.

3. CLOSED LOOP CONTROL DIAGRAM FOR ROTOR SIDE CONTROLLER:

In the RSC, the controller is used for controlling rotor power Ps and the power Qs in terms of controlling rotor regulation and rotating reference frame.

By considering the simplified equivalent circuit for stator winding as shown in figure 3 and write the equations by using KVL as

$$\bar{V}_r = \bar{I}_r R_r + \frac{d\psi_r}{dt} \quad (11)$$

$$\bar{\psi}_r = L_r \bar{I}_r + M \bar{I}_s e^{-j\in} \quad (12)$$

Substituting the value of $\bar{\psi}_r$ in above equation e get

$$\bar{V}_r = \bar{I}_r R_r + \frac{d}{dt}(L_r \bar{I}_r + \frac{M}{L_s}\bar{\psi}_s e^{-j\in} - \frac{M^2}{L_s}\bar{I}_r$$

$$= \bar{I}_r R_r + \frac{d}{dt}\left(L_r \bar{I}_r - \frac{M^2}{L_s}\bar{I}_r\right) + \frac{d}{dt}\left(\frac{M}{L_s}\psi_s e^{-j\in}\right)$$

Fig 5 shows the overall RSC control scheme which is having two cascade loops. The active and reactive powers of the DFIG is controlled by the outer loop and direct axis current component Idr*, quadrature axis current component Iqr* are generated. Inner-loop current regulation is the second cascaded control loop. Vdr0 and Vqr0 are the from the two regulated current controllers outputs. And these signals are used for generating Pulses to RSC converter by PWM technique.

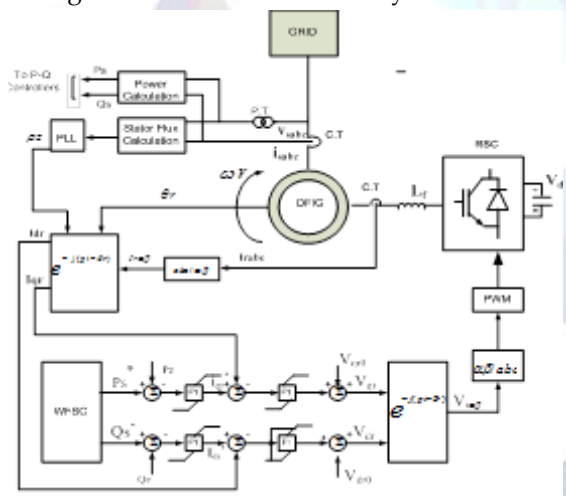

Figure 5: Control Diagram for the rotor side controller

4. CLOSED LOOP CONTROL DIAGRAM GRID SIDE CONVERTER:

Controlling of the reactive power Qg which is exchanged between the stator side converter and the grid with the help of dc link voltage is the complete control scheme for the GSC.

Form the equivalent circuit shown in figure 3. Applying KVL to above circuit we get

$$v_a = I_a R_f + L_f \frac{dI_a}{dt} + v_{ag} \quad (13)$$

$$v_b = I_b R_f + L_f \frac{dI_b}{dt} + v_{bg} \quad (14)$$

$$v_c = I_c R_f + L_f \frac{dI_c}{dt} + v_{cg} \quad (15)$$

Transform the above three phase coordinates in to two phase d-q transformation and separate real & imaginary terms we get

$$v_{sd} = I_{sd} R_f + L_f \frac{dI_{sd}}{dt} - w_s L_f I_{sq} + v_g$$

$$v_{sq} = I_{sq} R_f + L_f \frac{dI_{sq}}{dt} - w_s L_f I_{sd} \quad (16)$$

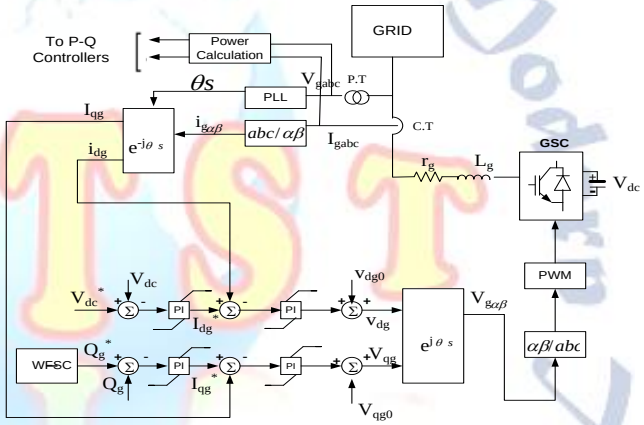

Figure 6: Grid side controller (GSC) scheme

Fig 6 shows the complete closed loop control diagram for the grid side converter and it having two cascaded control loops. The reactive power is indirectly controlled by the dc link voltage controlling done by the outer control loop for generating the reference signals of the d-axis current component idg* and q-axis current component iqg* for the inner-loop current regulation. Then these signals are used for generating pulses with the help of PWM technique

$$P_{ei,\max} = P_{mi,\max} - P_{Li} = P_{si,\max} + P_{ri,\max}$$

The stator active power Ps can be written as

$$P_s = \frac{3}{2}(v_{ds} i_{ds} + v_{qs} i_{qs}) = \frac{3}{2}[\omega_s L_m (i_{qs} i_{dr} - i_{ds} i_{qr}) + r_s (i_{ds}^2 + i_{qs}^2)]$$

The rotor side active power can be expressed

$$P_r = \frac{3}{2}(v_{dr} i_{dr} + v_{qr} i_{qr}) = \frac{3}{2}[-s\omega_s L_m (i_{qs} i_{dr} - i_{ds} i_{qr}) + r_r (i_{dr}^2 + i_{qr}^2)]$$

Artificial Neural Networks

Figure 7 shows the basic architecture of artificial neural network, in which an hidden layer is indicated by circle, an adaptive node is represented by square. In this structure hidden layers are presented in between input and output layer, these nodes are functioning as membership functions and the rules obtained based on the if-then statements is eliminated. For simplicity, we considering the examined ANN have two inputs and one output. In this network, each neuron and each element of the input vector p are connected with weight matrix W.

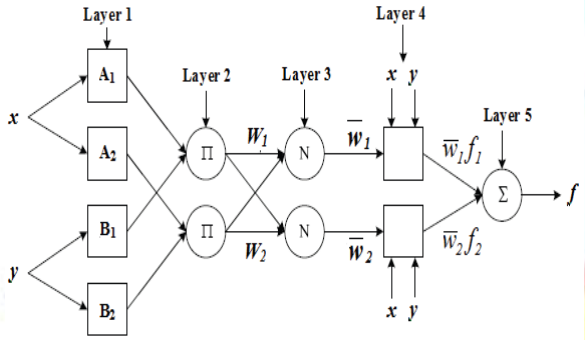

Figure 7: ANN architecture for a two-input multi-layer network

Where the two crisp inputs are x and y, the linguistic variables associated with the node function are Ai and Bi. The system has a total of five layers are shown in Figure 7.

Step by step procedure for implementing ANN:

1. Identify the number of input and outputs in the normalized manner in the range of 0-1.
2. Assume number of input stages.
3. Identify number of hidden layers.
4. By using transig and poslin commands create a feed forward network.
5. Assume the learning rate should be 0.02.
6. Choose the number of iterations.
7. Choose goal and train the system.
9. Generate the simulation block by using 'genism' command.

5. SIMULATION DIAGRAM AND RESULTS:

Here the simulation is done for maintaining the real power supplied by the wind farm is to be maintained constant. The constant real power is given as Pref to the wind turbines under different conditions like wind turbines operating without any energy storage system, operating with energy storage system with two-layer conventional controllers. The amount of real power that has to be maintained constant. The simulation diagram is shown in figure 8.

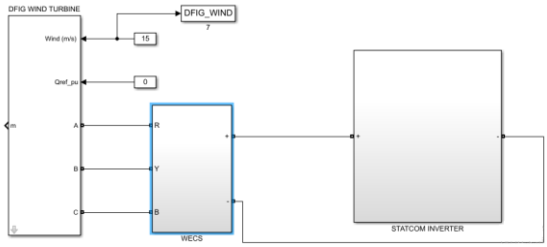

Figure 8: Simulation Diagram for DFIG WIND turbine

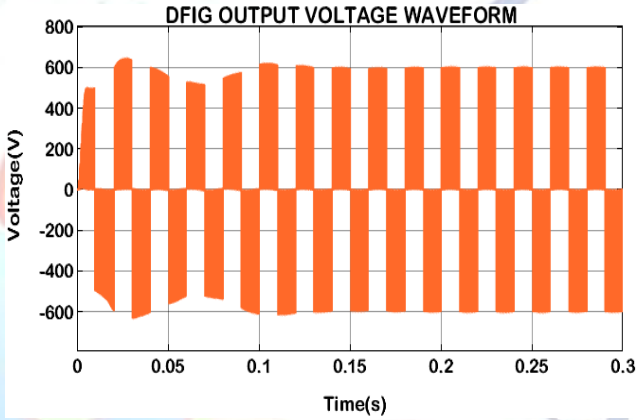

(a)

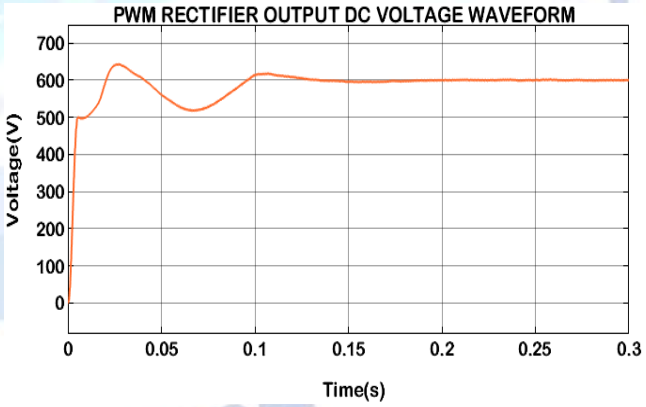

(b)

Figure 9: **(a)** DFIG based WECS output voltage and **(b)** PWM rectifier output voltage

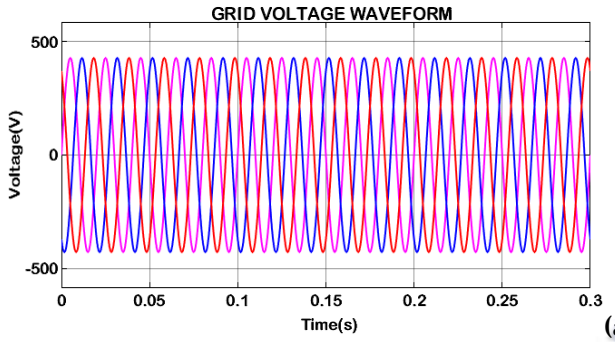

(a)

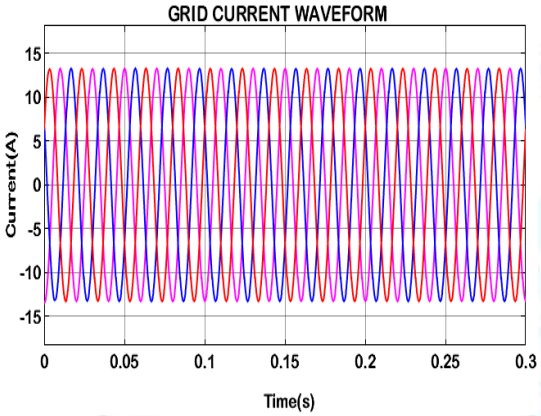

(b)

Figure 10: Waveforms of 3φ grid **(a)** Voltage and **(b)** Current

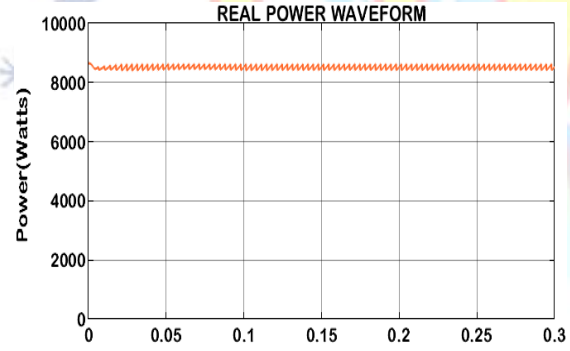

(a)

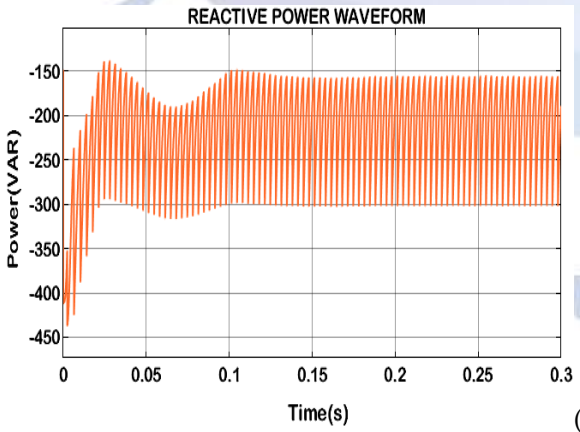

(b)

Figure 11: 3φ grid **(a)** Real power waveform and **(b)** Reactive power waveform

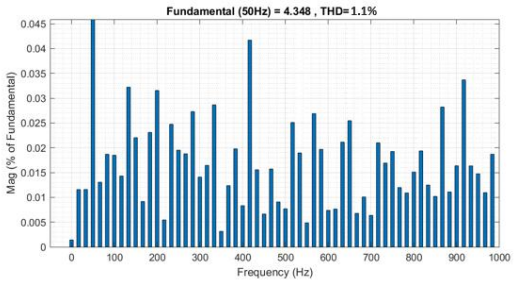

Figure 12: THD Waveform

6. CONCLUSION

This paper proposes a WECS system for reactive power compensation in distribution system by utilizing ANN controller. In this proposed method, Artificial Neural Network based D-Q theory extracts the reference current from source current for Harmonics and reactive power mitigation. The voltage from the WECS is fed to the dc-link of the DSTATCOM and the dc-link voltage is regulated and maintained stable using PI controller. In WECS, the ac output from wind turbine is converted into dc with the assistance of the PWM rectifier. The link voltage is fed to the grid via three phase inverter, which assists in DC-AC conversion and finally grid synchronization is achieved through DQ theory. The grid synchronization is achieved by synchronizing the inverter output current with injected grid voltage. The goal of synchronization algorithm is to extract the phase angle of grid voltage. The feedback values are transformed into an appropriate reference frame by utilizing extracted grid angle. A simulation model is created in MATLAB for the WECS system to examine its effectiveness.

Conflict of interest statement

Authors declare that they do not have any conflict of interest.

REFERENCES

[1] IEEE Std. 519-2014 (Revision of IEEE Std. 519-1992), IEEE Recommended Practice and Requirements for Harmonic Control in Electric Power Systems, DOI 10.1109/IEEESTD.2014.6826459, pp. 1–29, Jun. 2014.

[2] Y. J. Wang, R. M. O'Connell, and G. Brownfield, "Modeling and prediction of distribution system voltage distortion caused by nonlinear residential loads," IEEE Trans. Power Del., vol. 16, DOI 10.1109/61.956765, no. 4, pp. 744–751, Oct. 2001.

[3] Oraee, "A quantitative approach to estimate the life expectancy of motor insulation systems," IEEE Trans.

Dielectr. Electr. Insul., vol. 7, DOI 10.1109/94.891990, no. 6, pp. 790– 796, Dec. 2000.

[4] D. Fabiani and G. C. Montanari, "The effect of voltage distortion on ageing acceleration of insulation systems under partial discharge activity," IEEE Electr. Insul. Mag., vol. 17, DOI 10.1109/57.925300, no. 3, pp. 24–33, May. 2001.

[5] T. J. Dionise and V. Lorch, "Harmonic filter analysis and redesign for a modern steel facility with two melt furnaces using dedicated capacitor banks," in IEEE IAS Annual Meeting, vol. 1, DOI 10.1109/IAS.2006.256496, pp. 137–143, Oct. 2006.

[6] D. Ramirez-Castro, E. O'Neill-Carrillo, and J. Santiago-Perez, "Assessment of harmonics at a medical facility," in IEEE International Conference on Harmonics and Quality of Power, vol. 2, DOI 10.1109/ICHQP.2000.897750, pp. 619–624, 2000.

[7] U. Rao, S. N. Singh, and C. K. Thakur, "Power quality issues with medical electronics equipment in hospitals," in IEEE International Conference on Industrial Electronics, Control and Robotics, DOI 10.1109/IECR.2010.5720150, pp. 34–38, Dec. 2010.

[8] K. D. McBee and M. G. Sim˜oes, "General smart meter guidelines to accurately assess the aging of distribution transformers," IEEE Trans. Smart Grid, vol. 5, DOI 10.1109/TSG.2014.2320285, no. 6, pp. 2967– 2979, Nov. 2014.

[9] H. E. Mazin, E. E. Nino, W. Xu, and J. Yong, "A study on the harmonic contributions of residential loads," IEEE Trans. Power Del., vol. 26, DOI 10.1109/TPWRD.2010.2096236, no. 3, pp. 1592–1599, Jul. 2011.

[10] S. Munir and Y. W. Li, "Residential distribution system harmonic compensation using PV interfacing inverter," IEEE Trans. Smart Grid, vol. 4, DOI 10.1109/TSG.2013.2238262, no. 2, pp. 816–827, Jun. 2013.